Vol 17 No 10, October 2008
1674-1056/2008/17(10)/3655-07

Chinese Physics B

© 2008 Chin. Phys. Soc.
and IOP Publishing Ltd

Studies on odd-parity states of the Sm atom*

Guan Feng(关 锋), Dai Chang-Jian(戴长建)†, and Zhao Hong-Ying(赵洪英)

Key Laboratory of Display Materials and Photoelectric Devices, Ministry of Education, Tianjin 300191, *China*

School of Science, Tianjin University of Technology, Tianjin 300384, *China*

(Received 1 January 2008; revised manuscript received 25 April 2008)

Two-step excitation and ionization processes are used to detect Sm atoms in many excited states populated with tunable lasers. The wavelength of the first laser is tuned to the resonances from the Sm $4f^6 6s^2\ ^7F_J$ (J=0–6) states to many odd-parity states with different electronic configurations, where the atoms are detected by photoionization process using an ultraviolet laser with a wavelength of 355 nm. Precise measurements on the energy level and intensity for many Sm $4f^6$ 6s6p and $4f^5 5d6s^2$ states have been carried out. In a theoretical analysis on the spectral data, such as peak position, relative intensity, many transitions can be identified as the resonances from the Sm $4f^6 6s^2\ ^7F_J$ (J=0–6) states to the atomic states with $4f^6 6s6p$ and $4f^5 5d6s^2$ electronic configurations. This work also reports many spectral data on the odd-parity states that cannot be found in the literature.

Keywords: spectra of Sm atom, odd-parity excited state, photoionization detection
PACC: 3280, 3270

1. Introduction

In recent years, studies on highly-excited alkaline-earth atoms have gained dramatic progress in both experimental and theoretical aspects. The progress can be classified into electromagnetic effects on spectra,[1,2] autoionization spectra,[3,4] the dynamic characteristics of autoionization,[5] the autoionization detection,[6] and so on. However, studies on more complex atoms, such as the rare-earth atoms, are much less, especially those with complicated spectral structures. For the past decade, there have been a great number of investigations devoted to Yb,[7,8] La,[9,10] and Ce[11,12] atoms, while studies on Sm atoms are scanty. There are several possible reasons for this: (a) the Sm atom has seven isotopes; (b) its ground state consists of seven fine-structure levels. Moreover, unlike the heavier rare-earth atoms, such as Yb atom, the Sm atom only has a few electrons in the 4f sub-shell. Since the 4f electrons are much more active in the case of Sm atom, their excitation certainly makes the Sm spectrum much more complex than that of Yb atom. Although there are some data on low-excited states of the Sm atom,[13] the general information about the spectrum, such as relative intensities, is not available. More recently, there have been some new works on Sm atom, but they are only related to the even-parity excited states.[14,15] Based on the above facts, it is necessary to study the odd-parity excited states of Sm atoms. In this paper, the two-step photoionization excitation technique is employed to systemically measure the spectra of Sm odd-parity states with the $4f^6 6s6p$ and $4f^5 5d6s^2$ configurations, from which the various spectral data are obtained. With a detailed analysis on the data through the theoretical method, we not only identify lots of Sm odd-parity states, but also report many new spectral data which cannot be found in the literature.

In the following an introduction of the experimental details will be given in Section 2. The theoretical method will be given in Section 3. In Section 4 the experimental results and discussion are presented. Section 5 gives the main conclusions.

2. Experimental details

As shown in Fig.1, the experimental setup consists of three parts: the laser system containing a tunable dye laser pumped by a YAG laser; the vacuum chamber comprising an atomic oven and an microchannel plate (MCP) detector, and a data acquisition system. All the lasers used in the experiments

*Project supported by the National Natural Science Foundation of China (Grant Nos 10574098 and 10674102), and the Natural Science Foundation of Tianjin, China (Grant No 05YFJMJC05200).
†Corresponding author. E-mail: daicj@126.com

are manufactured by Quanta System: a Giant-770 Nd:YAG pulsed laser with pulse width 6–8 ns running at 20 Hz frequency and a D-100 dye laser with line width of 0.1 cm^{-1}. The data acquisition system includes a model 4121B Boxcar and a 9650A digital pulse generator from AMETEC controlled by a computer. In order to ensure the excitation sequence, the time delays between laser pulses, the gate of Boxcar and the pulse of electric field are carefully controlled. The Sm atom source is from an effusive atomic beam sprayed from a resistively heated oven in a vacuum chamber. The atomic beam is collimated and directed to a region between two electric field plates, 1 cm apart, where it is crossed perpendicularly by the two laser beams to avoid the Doppler broadening.

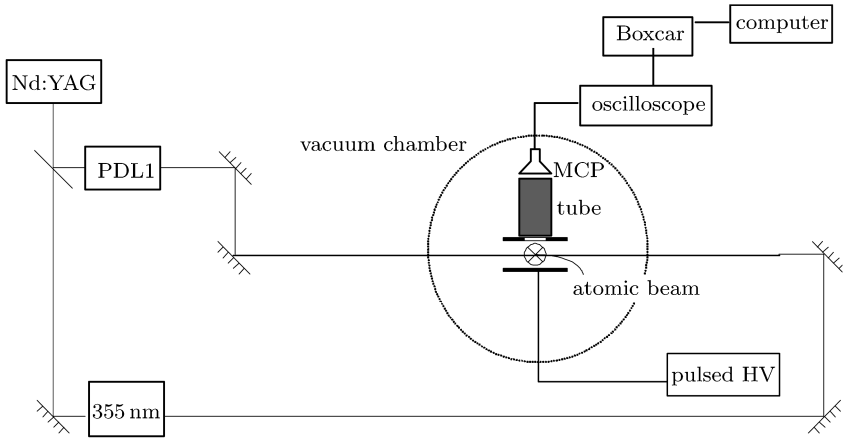


Fig.1. Schematic diagram of the experimental setup, which consists of laser, atomic beam , and data acquisition systems.

In order to fulfil the two-step excitation and photoionization scheme, as shown in Fig.2, two linearly polarized lasers are employed to interact perpendicularly with the Sm atomic beam, which is extracted from the stainless steel oven. The first laser, scanned within a certain wavelength range, excites an Sm atom from the $4f^6 6s^2\ {}^7F_{0-6}$ state to many states with $4f^6 6s6p$ or $4f^5 5d6s^2$ configuration.

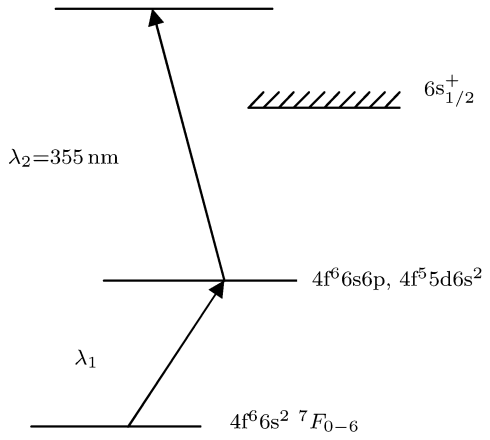


Fig.2. Illustration of the two-step excitation and ionization process. The Sm atoms in the $4f^6 6s^2\ {}^7F_{0-6}$ ground state are excited to states with the $4f^6 6s6p$ or $4f^5 5d6s^2$ configurations followed by photoionization.

The second laser whose wavelength is fixed at 355 nm makes a further step to detect the excited atoms by photoionizing them. About 500 ns after the laser pulses, a pulsed electrical field is used to push the ions to move towards the MCP detector so as to avoid the Stark effect in the process. The ion signals are integrated and averaged with a Boxcar, the output of which is stored in a computer for further analysis. To ensure the accuracy of the experiment, some efforts have to be made to reduce the possible errors. Specifically, a hollow cathode lamp and an F-P etalon are used for calibrating the laser wavelengths.

As described earlier, as long as the total energy of the two photons is set higher than the ionization limit of the Sm atom, the excited atoms can be detected. Note that the Sm atom has seven isotopes and seven fine-structure levels in its ground state. This causes following difficulties: (a) dilution of the transition probability for the Sm atoms makes the spectra more complicated; (b) several excitation routes occur in the same excitation scheme, leading to the mixed spectra originating from $3\lambda_1$, $\lambda_1+2\lambda_1$, $2\lambda_1+\lambda_1$ and so on.[16] Therefore, it is essential to differentiate and eliminate these disturbing signals. In other words, we

must control the timing, intensity, wavelength, and polarization of the laser pulses to guarantee that the signal comes from the unique excitation route. For example, it is useful to check the signal by tuning the first laser while fixing the second laser (detecting laser) at 532 nm. If there is no signal under this combination for photon energy while manipulating the intensities of two lasers, then with a detecting laser at 355 nm under the same condition we almost make certain that the signal originates from the atoms absorbing only one λ_1 photon. On the other hand, in order to make sure that Sm atoms are excited according to the excitation process shown in Fig.2, it is very important to control the time delay between the two laser pulses to delete some unwanted signals and to guarantee that the signals do come from both lasers, used.

3. Theoretical method

In the experiment, the Sm atoms in odd-parity states are detected in the photoionization process, results of which yield a great deal of information including level energy and relative intensity of spectral lines. By a detailed analysis of the observed spectra using the theoretical method, we not only identify many Sm atomic states but also obtain some new spectral data.

As we all know, the determination of wavefunctions of the Sm atom is a real many-body problem. Namely, the calculation on the transition matrix elements[17] is a very difficult task due to the complex structure of the Sm atom. Although the angular part of the wavefunction, related to l and m quantum numbers, can be determined, the radial part of it is difficult to calculate due to complicated form of the potential function.

Once the information about the potential function is available, the radial part of the wavefunction, in principle, can be obtained. If the atom is composed of N electronic configurations $(n_1l_1)^{N_1}(n_2l_2)^{N_2}....(n_rl_r)^{Nr}$, then the atomic Hamiltonian[18] can be expressed as

$$\hat{H} = -\sum_{i=1}^{N}\left(\nabla_i^2 + \frac{2z}{r_i}\right) + \sum_{i\neq j}\frac{2}{r_{ij}} + \sum_i \varepsilon_i(\boldsymbol{l}_i \cdot \boldsymbol{s}_i), \tag{1}$$

where r_i is the orbit radius of the ith electron, Z is the atomic number, r_{ij} is the distance between the ith electron and the jth electron, $\boldsymbol{l}_i$ and $\boldsymbol{s}_i$ are the orbit angular momentum and the spin angular momentum of the ith electron in the sub-shell (n_il_i) respectively. The energy of the atom can be written as $E = \sum_{i=1}^{N}\varepsilon_i$, where ε_i is the binding energy of single electron, and can be derived by the self-consistent theory.

In order to analyse the intensity of spectral lines, it is helpful to introduce the expression of the line intensity as[19]

$$I_{ki} = I_{ik} = \sum_{M_iM_k} |\langle kM_k\,|e\hat{\boldsymbol{r}}|\,\mathrm{i}M_i\rangle|^2. \tag{2}$$

Here, the degeneracy of energy levels is considered, and magnetic quantum numbers M_k and M_i correspond to k and i energy levels, respectively. It is evident that the line intensity can be evaluated once the wavefunctions are known. Usually, this requires an effective method for solving a many-body problem.[20] By separating the related electrons in a given system, a complex many-electron problem can be simplified to a single-electron problem and thus can be solved.[21,22]

With the known wavefunctions, one can rewrite the line intensity as

$$I = e\,\langle R_{\mathrm{e}}\,|\hat{\boldsymbol{r}}|\,R_{\mathrm{g}}\rangle\,\langle L'S'J'M'_J\,|\cos\theta|\,LSJM_J\rangle\,, \tag{3}$$

where R_{g} and R_{e} refer to the radial wavefunctions of the initial and the final states of Sm atom respectively, and $\langle L'S'J'M'_J\,|\cos\theta|\,LSJM_J\rangle$ is an angular integral. Using the well known expression

$$\begin{aligned}|LSJM_J\rangle &= \sum_{M_L,M_S} C(LSJ;M_LM_SM_J)\,|LSM_LM_S\rangle \\ &= \sum_{M_L,M_S}\begin{pmatrix} L & S & J \\ M_L & M_S & M_J\end{pmatrix}|LSM_LM_S\rangle\,,\end{aligned} \tag{4}$$

where $C(LSJ;M_LM_SM_J)$ is the Clebsch–Gordan coefficient, the integral can be calculated. It is important to point out that the calculation of spectroscopic data for Sm atom is one of the most complicated among the lanthanide atoms, due to the strong configuration mixing from the 4f electrons.

Since this experiment provide only the information of the relative intensity of spectral lines, the following theoretical analysis will only deal with the problem of relative intensity. According to the selection rules for the quantum number L, the line intensities can be classified into three cases, corresponding to $\Delta L = \pm 1$ and ΔL=0. However, since the intensities of a multiplet are determined by the levels between which the electron jumps and not by the direction of the jump, the line intensities for the $\Delta L = -1$ transitions can be determined if the line intensity for the

$\Delta L = 1$ transitions is known, using the symmetry between the initial state and the final state. Therefore, it is only necessary to list the formulas for the two cases corresponding to $\Delta L = 1$ and $\Delta L = 0$.[22] For each ΔL case, there are three values of ΔJ, so six formulas may be expected. For $\Delta L = 1$ case, we have[23]

a. $J - 1 \to J$

$$I = \frac{D(L+J+S+1)(L+J+S)(L+J-S)(L+J-S-1)}{J}; \tag{5}$$

b. $J \to J$

$$I = -\frac{D(L+J+S+1)(L+J-S)(L-J+S)(L-J-S-1)(2J+1)}{J(J+1)}; \tag{6}$$

c. $J + 1 \to J$

$$I = \frac{D(L-J+S)(L-J+S-1)(L-J-S-1)(L-J-S-2)}{J+1}. \tag{7}$$

Obviously, the common quantity D is not necessary to calculate if we only concern the relative intensity of spectral lines. For $\Delta L = 0$ case, we have[23]

d. $J - 1 \to J$

$$I = -\frac{E(L+J+S+1)(L+J-S)(L-J+S+1)(L-J-S)}{J}; \tag{8}$$

e. $J \to J$

$$I = \frac{E\left[L(L+1)+J(J+1)-S(S+1)\right]^2(2J+1)}{J(J+1)}; \tag{9}$$

f. $J + 1 \to J$

$$I = \frac{E(L+J+S+2)(L+J-S+1)(L-J+S)(L-J-S-1)}{J+1}. \tag{10}$$

Similarly, the common quantity E is also not necessary to calculate if we only concern the relative intensity of spectral lines.

4. Results and discussion

In this section we will display the experimental results and give a necessary analysis with the theoretical method described in the previous section. Figure 3 displays the ionization signals as a result of scanning the first dye laser in the wavelength range 442–465 nm when the second laser is set at 355 nm.

In the process of obtaining this spectrum, one must reduce the light intensity of the first laser to ensure no signal sent out while blocking the second laser. In addition, we carefully control the experimental settings in order to obtain the information about the relative intensity of spectral lines, which can be used as an additional tool for identifying transitions. For instance, the strongest line in Fig.3 can be identified as the transition from the $4f^6 6s^2\ {}^7F_0$ state to the $4f^5 5d6s^2\ {}^7G_1$ state. With a detailed analysis, one may recognize all the transitions in the spectrum, spectral data of which can be obtained as listed in Tables 1–3.

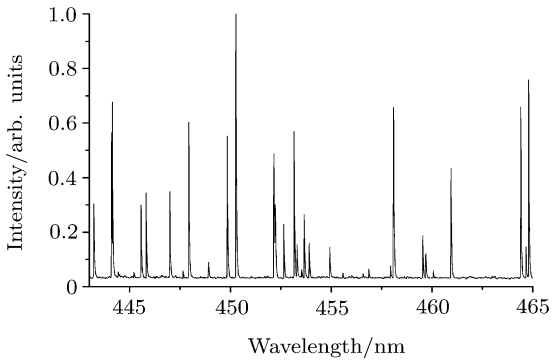


Fig.3. The Sm spectrum of the states with $4f^6 6s6p$ or $4f^5 5d6s^2$ configuration.

Figure 4 exhibits another spectrum of the excited states with $4f^6 6s6p$ or $4f^5 5d6s^2$ configuration. The experimental settings are the same as those used for the spectrum shown in Fig.3 except for sweeping the first laser from 485 to 530 nm. The spectral data of some identified transitions in this wavelength region are given in Tables 2 and 3. In order to obtain a

better spectral resolution, we not only carefully optimize the line-width of the laser, but also adopt a high-resolution rate of scanning.

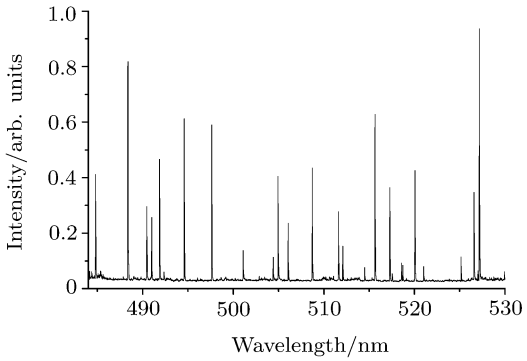


Fig.4. The Sm spectrum of the states with $4f^6 6s6p$ or $4f^5 5d6s^2$ configuration with longer wavelengths.

As mentioned above, because energy structures of Sm atoms are extraordinarily complicated, the thermal population introduces many disturbing signals in the spectra. Therefore, we have to make a great effort to distinguish these disturbing signals in order to obtain exact information about the Sm atom. Figure 5, for instance, shows a spectrum obtained by scanning the first laser alone from 480 to 500 nm without a detection laser. The wavelengths of four peaks in Fig.5 indicate that Sm atoms must be ionized by absorbing three photons from the same laser.[24]

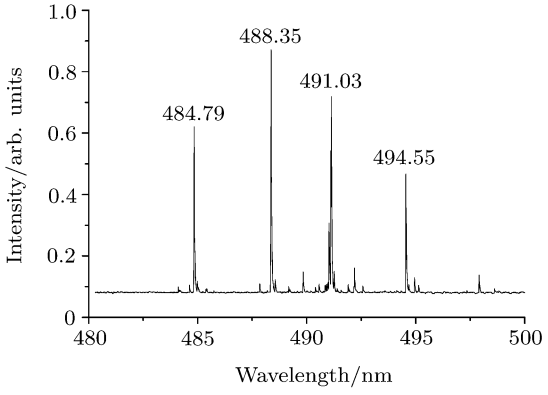


Fig.5. A portion of the single-colour three-photon resonance spectrum of the Sm atom.

Keeping the above fact in mind, we have to carefully control the light intensity of the first laser to make the signals shown in Fig.5 disappear. Furthermore, as described in Section 2, we have to use a 532 nm photon instead of 355 nm photon as our λ_2 in order to check and avoid the signals from $2\lambda_1 + \lambda_2$ process. With the above confirmation, it is certain that signals shown in both Figs.3 and 4 are from the $\lambda_1 + \lambda_2$ process only.

Now, let us turn to discuss the spectral data in Tables 1 to 3, which are tabulated according to the J value of the initial states of transitions. With the selection rules of both parity and angular momenta of a transition as well as a reliable calibration on wavelength as stated in Section 2, we are able to identify the states with configurations $4f^6 6s6p$ and $4f^5 5d6s^2$ of Sm atoms by matching the wavelengths of transitions. In addition, the relative intensities of transitions also enable us to recognize some spectral lines. In all the tables shown below, the uncertainty of wavelengths is ± 0.01 nm, and the relative intensity is normalized and classified into three ranges: 0–0.3, 0.3–0.6, and 0.6–1, marked by A, B and C, respectively.

Table 1 contains the spectral data for five possible transitions from the same initial state. As the $J = 0 \rightarrow J = 0$ transition is forbidden, for an Sm atom in $4f^6 6s^2\ ^7F_J$ (J=0) state only states with angular momentum J=1 are accessible. Although these transition lines can be deduced from the selection rules, their intensities are quite different. For instance, the expectation that transition satisfying $\Delta L = \Delta J$ should have a higher intensity is confirmed by the fact that the intensity of the transition to the $4f^5 6s6p\ ^7G_1$ state is much higher than that to the $4f^6 6s6p\ ^7F_1$ state.

Table 1. The observed spectra from the $4f^6 6s^2\ ^7F_0$ state providing information on wavelength, intensity, and energy levels.

λ_1/nm	Label	E/cm^{-1}	Intensity
430.09	$4f^5 5d6s^2\ ^7G_1$	23243.84	B
436.27	$4f^6 6s6p\ ^7G_1$	22914.07	B
448.01	$4f^6 6s6p\ ^7F_1$	22313.63	A
497.58	$4f^5 5d6s^2\ ^5F_1$	20091.03	B
526.57	$4f^6 6s6p\ ^5F_1$	18985.70	B

Let us see a more complicated situation as shown in Table 2, where spectral data of 11 possible transitions to states with $4f^6 6s6p$ or $4f^5 5d6s^2$ configurations from the same $4f^6 6s^2\ ^7F_1$ state are listed.

Table 2. The similar information to that in Table 1, but for the transitions from the $4f^6 6s^2\ ^7F_1$ initial state.

λ_1/nm	Label	E/cm^{-1}	Intensity
432.97	$4f^5 5d6s^2\ ^7G_2$	23380.75	*C*
435.57	$4f^5 5d6s^2\ ^7G_1$	23243.84	*B*
441.92	$4f^6 6s6p\ ^7G_1$	22914.07	*B*
450.32	$4f^5 5d6s^2\ ^5G_2$	22491.94	*C*
464.52	$4f^6 6s6p\ ^7D_2$	21813.22	*C*
478.28	$4f^6 6s6p\ ^7D_1$	21193.68	*C*
504.94	$4f^5 5d6s^2\ ^5F_1$	20091.03	*B*
515.72	$4f^6 6s6p\ ^5F_2$	19677.46	*B*
534.81	$4f^6 6s6p\ ^5F_1$	18985.70	*B*
554.86	$4f^5 5d6s^2\ ^7F_0$	18309.02	*B*
570.67	$4f^6 6s6p\ ^7F_0$	17810.85	*B*

It is very helpful to check the experimental results by calculating the line intensity according to the theory described in Section 3. For example, if we let I_1 denote the line intensity to the $4f^5 5d6s^2\ ^5G_2$ state (L=4, S=2, J=2) and I_2 denote the line intensity to the $4f^6 6s6p\ ^7G_1$ state (L=4, S=3, J=1), then Eqs.(5) and (6) in Section 3 yield I_1=432D, and I_2=162D, respectively. Obviously, the theoretical values agree well with the experimental results shown in Table 2.

When the initial state of the excitation has a higher J value, the situation is getting more complicated. There are 14 possible transitions from the $4f^6 6s^2\ ^7F_2$ state, spectral data of which are listed in Table 3. We have carried out a similar calculation, as for Table 2, and again the theory agrees well with the measurements. Specifically, let I_3 be the intensity of the transition $4f^6 6s^2\ ^7F_2 \rightarrow 4f^6 6s6p\ ^5F_3$ (L=3, S=2, J=3), and I_4 be the intensity of the transition $4f^6 6s^2\ ^7F_2 \rightarrow 4f^5 5d6s^2\ ^7F_2$ (L=3, S=3, J=2). Equations (8) and (9) in Section 3 yield the results matching the relative intensities listed in Table 3.

Table 3. Information for the transitions from the $4f^6 6s^2\ ^7F_2$ state.

λ_1/nm	Label	E/cm^{-1}	Intensity
442.94	$4f^5 5d6s^2\ ^7G_2$	23380.75	*C*
445.65	$4f^5 5d6s^2\ ^7G_1$	23243.84	*B*
452.29	$4f^6 6s6p\ ^7G_1$	22914.07	*B*
458.13	$4f^6 6s6p\ ^7D_3$	22632.30	*B*
461.11	$4f^5 5d6s^2\ ^5G_2$	22491.94	*B*
478.59	$4f^5 5d6s^2\ ^5F_3$	21700.89	*B*
490.48	$4f^6 6s6p\ ^7D_1$	21193.68	*B*
508.83	$4f^6 6s6p\ ^5F_3$	20459.30	*B*
518.56	$4f^5 5d6s^2\ ^5F_1$	20091.03	*B*
527.14	$4f^5 5d6s^2\ ^7G_3$	19776.97	*C*
534.92	$4f^5 5d6s^2\ ^7F_3$	19501.27	*A*
556.12	$4f^5 5d6s^2\ ^7F_2$	18788.08	*A*
565.96	$4f^5 5d6s^2\ ^7F_1$	18475.28	*B*
574.63	$4f^6 6s6p\ ^5G_3$	18209.04	*C*

For the information of spectral lines excited from the $4f^6 6s^2\ ^7F_3$ state and from the $4f^6 6s^2\ ^7F_4$ state, they are given in Tables 4 and 5, respectively. For Table.4, we take two lines as an example to check the results. Let I_5 represent the line intensity of the transition to the $4f^5 5d6s^2\ ^7G_3$ state (L=4, S=3, J=3) and I_6 represent the line intensity of the transition to the $4f^5 5d6s^2\ ^7G_2$ state (L=4, S=3, J=2), then Eqs.(6) and (7) in Section 3 provide the calculated results which agree with the measurements.

Table 4. For the transitions from the $4f^6 6s^2\ ^7F_3$ state.

λ_1/nm	Label	E/cm^{-1}	Intensity
447.03	$4f^5 5d6s^2\ ^7G_3$	23852.43	*B*
453.21	$4f^5 5d6s^2\ ^7G_2$	23546.54	*A*
467.07	$4f^5 5d6s^2\ ^5F_4$	22893.05	*B*
472.82	$4f^6 6s6p\ ^7D_3$	22632.30	*B*
491.87	$4f^6 6s6p\ ^7D_2$	21813.22	*B*
494.61	$4f^5 5d6s^2\ ^5F_3$	21700.89	*C*
518.70	$4f^5 5d6s^2\ ^5F_2$	20762.82	*B*
555.01	$4f^5 5d6s^2\ ^7F_3$	19501.27	*B*
564.72	$4f^6 6s6p\ ^7F_4$	19191.64	*C*

If we use the data in Table 5 as an example, it is interesting to confirm that the ΔS=0 rule is no longer valid for the Sm atom, indicating a strong effect from orbit-spin couplings. Examination of Tables 1–5 indicates that the $4f^6 6s6p\ ^5F_3$ state is always excited, although atoms are in different initial states, as shown in Tables 1–5. On the other hand, this fact can be turned into a tool for verifying the consistency of the present experiment by examining the same final state from many different initial states. If the measured wavelengths and relative intensities are all in accordance with the theoretical results, then one may be confident that the experimental results on spectral data are entirely reliable.

Table 5. From the $4f^6 6s^2\ ^7F_4$ state, the observed spectra provide information on wavelength, intensity, and energy levels.

λ_1/nm	Label	E/cm^{-1}	Intensity
453.36	$4f^6 6s6p\ ^7D_5$	24323.51	*C*
468.84	$4f^6 6s6p\ ^7D_4$	23594.84	*C*
484.81	$4f^5 5d6s^2\ ^5F_4$	22893.05	*C*
511.72	$4f^6 6s6p\ ^5F_5$	21809.74	*B*

Finally, it is important to point out that many transition spectral lines observed in the present work may be not found in the literature. Their spectral information, including transition wavelength, relative intensity, and spectral designations are not available.

In order to eliminate any possibility of accidental excitation by one laser alone, we have performed many tests to confirm that all the ionization signals originate from the $\lambda_1 + \lambda_2$ process. At the same time, we have carried out the experiments to verify the spectral data over and again to ensure that the data reported here are genuine. The final experimental results are tabulated in Table 6, including the transition wavelength and line intensity.

Table 6. Wavelength and intensity of transitions from the ground state to the odd-parity excited state.

λ_1/nm	Intensity	λ_1/nm	Intensity
418.43	*C*	453.73	*B*
421.91	*B*	454.98	*A*
428.32	*B*	459.65	*A*
429.89	*C*	471.84	*B*
431.36	*A*	476.00	*C*
431.92	*B*	504.41	*A*
432.42	*A*	512.19	*A*
433.89	*C*	525.16	*A*
435.05	*B*	551.58	*B*
443.28	*B*	557.47	*C*
444.22	*B*	562.13	*B*
445.90	*B*	564.14	*A*
449.87	*B*	565.26	*A*
452.23	*B*	567.84	*B*
452.71	*A*	574.08	*B*

Since the data shown here have never been reported, we believe that they come from the transitions of the 4f electrons. The electrons in the sub-shell are quite active, and are easily excited by a photon with a visible wavelength. For this reason, their excitation may heavily disturb the transitions of valance electrons in the outer shell, leading to a complex spectrum. To obtain a best understanding about these spectral data and to label these transition to certain final states correctly it is necessary to carry out a comprehensive theoretical study.

5. Conclusions

A systematic study on the odd-parity excited states of Sm atom has been carried out with two-step excitation and photoionization. The energy levels of many odd-parity excited states with the $4f^6 6s6p$ and $4f^5 5d6s^2$ configurations excited from different initial states have been identified. The relative intensities of these transitions have been measured, which agree well with the theoretical results. In addition, many new spectral data, including the transition wavelength and relative intensity, are obtained. Their spectral identification requires a more detailed theoretical study.

References

[1] Liu Y P, Dai C J and Li S B 2005 *J. Electron Spectrosc. Related Phenom* **142** 91

[2] Liu H P, Quan W, Shen L, Connerade J P and Zhan M 2007 *Phys. Rev.* A **76** 013412

[3] Li S B and Dai C J 2007 *Chin. Phys.* **16** 2

[4] Zhang Y, Dai C J and Li S B 2005 *J. Electron Spectrosc. Related Phenom* **148** 11

[5] Li S B, Dai C J and Zhang Y 2002 *Chin. Phys.* **11** 690

[6] Zhi M C, Dai C J and Li S B 2001 *Chin. Phys.* **10** 929

[7] Biemont E, Quinet P, Dai Z W, Jiang Z K, Zhang Z G, Xu H L and Svanberg S 2002 *J. Phys.* B: *At. Mol. Opt. Phys* **35** 4743

[8] Biemont E, Garnir H P, Lokhnygin V, Palmeri P, Quinet P, Svanberg S, Wyart J F and Zhang Z K 2001 *J. Phys.* B: *At. Mol.Opt. Phys* **34** 1869.

[9] Sun W, Xue P, Xie X P, Huang W, Xu C B, Zhong Z P and Xu X Y 2001 *Phys. Rev.* A **64** 031402(R)

[10] Sun W, Yan J, Zhong Z P, Xie X P, Xue P and Xu X Y 2001 *J. Phy.* B: *At. Mol. Opt. Phys.* **34** 369

[11] Cheal B, Avgoulea M, Billowes J, Campbell P, Flanagan K T, ForestD H, Gardner M D, Huikari J, Marsh B A, Nieminen A, Thayer H L, Tungate G and Äystö J 2003 *J. Phy.* G: *Nucl. Part. Phys.* **29** 2479

[12] Li G S, Meng R and Zhu L H 2004 *Chin. Phys. Lett.* **21** 46

[13] Martin W C, Zalubus R and Hagan L 1978 *Atomic Levels—the Rare-Earth Elements* Natl. Bur. Stand., USA, Circ 60

[14] Kondo T, Angom D, Endo I, Fukumi A, Horiguchi T, Iinuma M and Takahashi T 2003 *Eur. Phys. J.* **25** 103

[15] Jayasekharan T, Razvi M A N and Bhale G L 2000 *J. Phys.*B: *At. Mol. Opt. Phys.* **33** 3123

[16] Gomonai A I and Kudelich O I 2002 *Optics and Spectroscopy* **93** 198

[17] Connerade J P 1988 *Highly Excited Atoms* (London: Cambridge University Press)

[18] Mou Z D and Wei Q Y 2004 *Acta Phys. Sin.* **44** 1742 (in Chinese)

[19] Celik G and Ates S 2007 *Eur. Phys. J.* **44** 433

[20] Zheng N W, Zhou T, Wang T, Yang R Y, Sun Y J, Wang F and Chen C G 2002 *Phys. Rev.* A **65** 052510

[21] Zheng N W, Sun Y J and Ma D X 2001 *Int. J. Quant. Chem.* **81** 232

[22] Fan J, Zheng N W, Ma D X and Wang T 2004 *Phys. Scr.* **69** 398

[23] Lin M R and Zhang B Z 1990 *Introduction to Atomic Spectra* (Beijing: Science Press of China) (in Chinese) 140

[24] Gomonai A I and Plekan O I 2003 *J. Phys.* B: *At. Mol. Opt. Phys.* **36** 4155